BUCHAREST CYCLOTRON AS INTENSE FAST NEUTRON SOURCE FOR RADIOBIOLOGICAL AND ANALYTICAL APPLICATIONS

B. CONSTANTINESCU, M. MACOVEI, T. PAUNICA, S. DIMA, R. BUGOI, C. GARLEA, I. GARLEA, V. LABAU, L. RADU AND A. SASIANU

Institute of Atomic Physics, PO BOX MG-6, Bucharest, Romania

Due to interest for applications in radiobiology and material testing, Bucharest U-120 classical variable energy Cyclotron is employed as an intense source of fast neutrons, using 13.5 MeV deuterons bombarding a Beryllium target placed at 20° against the incident beam. Energy spectra, yields, average energy and irradiation doses were determined using time-of-flight (TOF), multiple foils and thermoluminescent detectors (TLD) methods. The average energy is 5.24 MeV. The total yield at 0°, obtained by summing up the yields for neutron energies between the lower (0.3 MeV) and upper (17 MeV) thresholds, is 6.7×10^{16} n/sr·C·MeV. The yield of the low energy component (0.3-2 MeV) is 1.88×10^{16} n/sr·C·MeV, i.e. 28% of the total yield at 0°. We present studies on the influence of thyotepa, thyroxine, metallic ions (Cs^{1+} and Al^{3+}) and D_3 vitamin on fast neutron radiolysis in tumor DNA and conclusions on the role of thyotepa (accelerator for tumor destruction) and of tyroxine, metallic ions and D_3 vitamin (protectors). The potential for elemental analysis, especially for light elements (O, Na, Mg, Al, Si) on archaeological glass and ceramics objects is discussed.

1 Time-of-flight measurements

To produce fast neutrons at our U-120 classical variable energy Cyclotron, deuterons accelerated up to 13.5 MeV bombard a thick (166.5 mg/cm^2) Beryllium target placed at 20° against the incident beam [1]. For TOF measurements, with a Ta-slit of 8 mm diameter and an electrode electron suppression, the beam currents on the target were no more than 5-15 nA, in order to avoid large dead-time values, while the current on the slit was kept lower than 0.5 nA. Target beam currents with appropriate electron suppression were integrated to determine the incident particle beam charge. The collimators are arranged so those only neutrons originating from the target are detected, while the neutrons originating from the beam tube do not reach the detector. The neutron detectors consisted of two NE 102 scintillators of 40-mm diameter and 60 mm thick coupled to 56 AVP photomultipliers. One of them was placed at fix angle of 90° for an additional monitoring. The flight path was of 4.5 m. The detection threshold was set at 0.3 MeV. The calibration of the spectrometer was performed with standard gamma sources. The existing data [2] concerning the light output of the plastic scintillator NE 102 to electrons and protons were used to find the equivalent neutron energies. The intrinsic efficiency of the detector corresponding to 0.3 MeV threshold energy was calculated using the code elaborated by Kurz [3], in which the composition of NE 102 scintillator as well as more recent cross section data were introduced in calculations.

As the expected energy range of neutrons was from 0.3 MeV to 17 MeV, a larger time separation is required between the two successive beam pulses on the target, in order to avoid overlapping of the rapid neutrons with the slow neutrons coming from the previous period. Therefore, the frequency of the beam pulses on the target was 1.26 MHz, i.e. one ninth of the nominal cyclotron frequency, assuring a convenient time range of the analysis (925 ns). According to the usual procedure, the time-of-flight spectra were converted into the energy scale and corrected for dead-time, background contribution and detector efficiency. Finally, the neutron yield in units of n/steradian·C·MeV was calculated averaging over 0.2 MeV energy intervals.

Energy spectra of neutrons emitted at angles between 0° and 120° were measured. The background was determined in separate measurements with a paraffin block placed between the target and the detector. A peak is clearly seen at 0.6 MeV neutron energy in agreement with Lone et al. [4], who explained it by the decay of Be states excited from direct inelastic reactions. The presence of a low energy component is observed in agreement with other measurements at close bombarding energies, reflecting the contributions of many mechanisms to the emission of neutrons: compound nucleus formation, excitation of ^{9}Be states, etc.

All measured spectra presented a non-negligible component above the cinematically allowed limit. Energy considerations led us to the conclusion that this is due to aluminum impurities possibly present in the Beryllium target. For extracting this contribution, neutron spectra produced by 13.5 MeV deuterons on an Al target of 13.5 mg/cm^2 were determined in a separate measurement.

The average energy for thick Be target and for neutron energies above 0.3 MeV is 5.24 MeV. The total yield at 0° obtained by summing up the yields for neutron energies between the threshold (0.3 MeV) and 17 MeV is 6.7×10^{16} n/sr·C·MeV. The yield of the low energy component (0.3-2 MeV) is 1.88×10^{16} n/sr·C·MeV; this value represents 28% of the total yield at 0°, being in good agreement with data from [4]. The angular distribution of the neutrons are strongly forward peaked, reflecting the presence of a direct mechanism (from 6.7×10^{16} n/sr·C·MeV at 0° to 1.3×10^{16} n/sr·C·MeV at 40°).

2 Multiple foils method (activation detectors and fission chambers)

Neutron characterization in the range 10^{-10}-18 MeV was performed by multiple foils method (activation

detectors and fission chambers), both in free-air, at 5 cm behind Be target, and in the irradiation space (a 0.02m thick wall wood box, $0.3 \times 0.3 \times 0.3 m^3$, surrounded by 0.5 m paraffin and placed on a 0.7 m limonite concrete pedestal base), at 10 cm behind Be target, on the geometrical axis of the neutron "beam" ($0°$). 10 μA of 13.5 MeV deuteron beam was employed to produce intense neutron fields suitable for the method. Six activation detectors (metallic foils as sandwiches): $^{115}In(n,n')^{115}*In$ ($E_{threshold}=0.6$ MeV), $^{59}Co(n,\alpha)^{56}Mn$ ($E_{threshold}=0.3$ MeV), $^{24}Mg(n,p)^{24}Na$ ($E_{threshold}=6.4$ MeV), $^{27}Al(n,\alpha)^{24}Na$ ($E_{threshold}=6.6$ MeV), $^{56}Fe(n,p)^{56}Mn$ ($E_{threshold}=5.7$ MeV), $^{58}Ni(n,p)^{58}Co$ ($E_{threshold}=1.9$ MeV) and an absolute calibrated fission chamber type Saclay [5] containing ^{235}U, ^{239}Pu, ^{238}U, ^{237}Np, ^{232}Th were simultaneously irradiated surrounded by 1 mm Cd foil. As permanent monitors, in the same plane with the detectors, at $120°$ (6cm distance to $0°$ axis), three absolute calibrated fission chambers ($^{238}U+1\%^{233}U$, $^{238}U+1\%^{239}Pu$, $^{238}U+400ppm^{235}U$) were used. The absolute determination of the fission rates was performed using J. Grundl's procedure [6]. The activation rates were determined by high resolution gamma spectrometry, using a 100 cc Ge(Li) detector, calibrated in absolute efficiency. Experimental corrections for fission chamber measurements were dead-time, fissionable impurities in deposits, extrapolation to zero (ETZ), absorption of fission fragments in deposits.

The neutron spectrum was obtained from the absolutely measured reaction rates by means of SANDII code [7], using an unfolding procedure. The input was built as follows:

-[0 keV...300 keV]-1/E extrapolation;

-[300 keV...17.2 MeV]-the spectra obtained using TOF method;

-above 17.2 MeV-fusion spectrum.

The used cross sections are gathered in the Dosimetry file of ENDF/B V library. In figure 1 are presented the neutron spectra in the range of 300 keV-18 MeV for free-air (5 cm behind the target) and for irradiation box (10 cm behind the target), normalized in order to be compared with the TOF spectrum. In the case of free-air, above 8 MeV the values obtained by unfolding are greater than those determined by TOF, but below 3 MeV, the values obtained by SANDII code are less than those measured using TOF. The integral flux in the range 0-300 keV obtained by unfolding is approximately 1% from the total flux for free air, but 5% in the case of irradiation box. For free-air (5 cm behind Be target), the absolute intensity flux is $6.63 \times 10^8 n/cm^2 \cdot \mu C$ and for irradiation box (10 cm behind Be target) $2.13 \times 10^8 n/cm^2 \cdot \mu C$. The average energy of the neutron spectrum in the range 0.3 - 17 MeV (free-air), determined by unfolding, is 5.352 MeV. Due to the experimental errors (4-5%) and to the limited precision (5-15%) of cross section values, incertitude in the range of 8-20% is estimated for the spectral shape.

3 Measurements using gamma and gamma + neutron thermoluminescent detectors

To determine neutron and gamma irradiation doses, home made (Institute of Atomic Physics) thermoluminescent detectors - TLD (γ) and TLD (γ+n)-were used: for gamma MgF_2: Mn mixed with Teflon pellets (ϕ 12.5 mm, 0.6 ± 0.1 mm thick) and for gamma plus neutrons MgF_2: Mn mixed with ^6LiF and Teflon pellets (same dimensions) [8]. Detector gamma sensitivity was determined using calibrated ^{60}Co sources ($S_\gamma=85.0$ impulses/Gy(γ)). Thermal neutrons sensitivity was measured irradiating both gamma and gamma + thermal neutrons TLDs in a calibrated thermal channel of the Bucharest VVRS Reactor ($S_n = 21.01$ Gy(γ)/Gy(n), where 1 Gy(n)=$3 \cdot 10^{11}$ thermal neutrons/cm^2).

Both TLD (γ) and TLD (γ+n) were placed in our mixed γ+n field at 10 cm behind the Be target on a phantom (a tissue equivalent sphere of 30 cm diameter)-in similar radiobiological irradiation conditions. Thermoluminescent parameters were measured using a Victoreen 2800 apparatus. So, the difference between TLD (γ+n) and TLD (γ) values is due to the thermalized and backscattered from phantom neutrons (albedo effect). To calibrate the procedure, $^{115}In(n,n')$ activation detectors (indium foils) were simultaneously irradiated with the TLDs to measure the total neutron fluency, using spectrum information previously obtained from activation foils method. The thermal neutron fluency was determined from the above mentioned dose difference using 1 Gy(n)=$3 \cdot 10^{11}$ thermal neutrons/cm^2 equivalence. The ratio thermal fluency/total fluency gives the albedo factor (in our case $8.022 \cdot 10^{-2}$) for the specific neutron spectrum at our Cyclotron.

In a concrete radiobiological irradiation, a TLD (γ) plus TLD (γ+n) pair is placed near the sample and the thermalized neutron fluency is determined as above. Using the previous albedo factor value and the equivalence 1 Gy(n)=$2 \cdot 10^{10}$ fast neutron/cm^2, the dose for the irradiation is found, with an estimated precision of 15%. Values of $1.2 \cdot 10^{-2}$ Gy/μC for neutrons and $7.8 \cdot 10^{-4}$ Gy/μC for gamma at 10 cm behind Be target and $0.38 \cdot 10^{-4}$ Gy/μC for gamma at 100 cm behind Be target were determined.

4 Studies on chromatin structure modifications

The growing interest in neutron therapy requires complex studies on the mechanisms of neutron action on biological systems, especially on chromatin (the complex of deoxyribonucleic acid-DNA with proteins in eukaryotic cells). We extracted the chromatin from normal tissue-livers of Wistar rats-and from tumoral tissue-Walker tumor maintained on Wistar rats [9]. For chromatin separation, we used supplementary nuclei purification through a passage on 1 M sucrose and we verified the obtained purity by an absorption test. Suspensions of cells-5×10^6 cells/ml

concentration-from Wistar rat livers and from Walker tumors were also isolated. We used irradiation doses from 5 Gy to 100 Gy. The dose contribution of gamma photons was about 10%. The dose mean lineal energy in water at the point of interest was 50 keV/μm. The mean dose rate was 1.5 Gy/min. To study the post-irradiation effects, various methods such as chromatin thermal transition (E_0-before and E-after transition), chromatin-ethidium bromide complex fluorescence and intrinsic chromatin fluorescence for tyrosine (specific for basic proteins) and for tryptophane (specific for acid proteins) were employed. For normal chromatin, we observed a diminution of the negative fluorescence intensity for chromatin-ethidium bromide complexes with the increase in neutron dose (from 0.98 at 5 Gy to 0.85 at 100 Gy). This fact reflects chromatin DNA injuries, with the decrease of double helix DNA proportion. As is known, single and double strand breaks are produced under fast neutron action. The quantity of the remaining DNA double strand, determined by fluorimetric analysis of the unwinding DNA, also decreased with neutron dose. We also observed a reduction of intrinsic fluorescence intensities with neutron dose (approximately 1.5 times from 5 to 100 Gy), denoting a destruction of chromatin proteins structure. The energy transfer efficiency also decreased under neutron action (from 0.224 at 5 Gy to 0.135 at 100 Gy), indicating a more unstable tertiary structure of chromatin.

To study the influence of thyotepa, thyroxine and D_3 vitamin treatments on fast neutron radiolysis in tumor chromatin, we administrated, separately or associated, to Wistar rats bearing Walker carcinosarcoma 10 mg/kg of anticancer drug thyotepa, 40 μg/kg of hormonal compound thyroxine and 30,000 UI/kg of D_3 vitamin. We performed similar studies on chromatin modifications as mentioned above. The treatment with thyotepa accelerates the damage processes, but adding tyroxine and D_3 vitamin, the negative effects are partially recuperated. Some conclusions on the role of thyotepa (as accelerator for tumor destruction) and of tyroxine and D_3 vitamin (as protection) are evident. Such results could constitute an indicator for associated chemotherapy-radiotherapy scheduled in clinical applications.

5   Archaeometrical studies

The potential for light elements (O, Na, Mg, Al, and Si) was for the first time presented in [10]. In the frame of our archaeometrical program for Byzantine objects (coins, glasses, ceramics) we used FNAA as a complementary method to XRF (X-Ray Fluorescence) and PIXE (Particle Induced X-ray Emission). FNAA is a non-destructive bulk analytical tool and the objective is to determine some light elements (Na, Mg, Al, Si, K), to solve the problem of interference (X-rays) in the case of As-Pb and to explore its possibilities for other major, minor and trace elements. We irradiated some Cu and Pb coins, glass and ceramics samples placed at 5 cm behind the Be target

for 100 minutes with a current beam intensity of 8-9 μA (Q=50 mC, corresponding to 5×10^{12} n/cm^2). The radioactivity was measured in two stages: after 30 min cooling time (Si, Al, Mg, K are determined - see Table 1) and after 72 h cooling time -for the rest of radioisotopes (see also Table 1). We used an Ortec HPGe detector (1.9 keV resolution at 1332.5 keV and 25% relative efficiency), connected to an 8192 channels Spectrum 88 MCA. The samples were put at 3-5 cm in front of detector.

Because the broad energy spectrum (see Fig.1), nuclear reactions such as (n,γ), (n,2n), (n,p), (n,α) are easily produced but the interference must be considered. The threshold values for (n,2n) nuclear reactions are of the order of 10 MeV and taking into account the fact that there are very few neutrons with so high energy, we observed only the reaction on Ca, As, Ag, Sb. For the Cu coins we detected radioisotopes from Fe, Ni, Cu, Zn, As, Ag, Sn, Sb, Pb; for the Pb coins: Fe, Cu, Zn, As, Ag, Cd, In, Sn, Sb, Pb (interference In-Sn, Cd-In); for ceramics: Mg, Al, Si, K, Ca, Ti, Fe, Zr, Ba, Ce (interference Mg-Al-Si, Y-Zr) and for glass: Na, Mg, Al, Si, K, Ca, Fe, Cu, Zn, As, Ba, Ce, Pb (interference Na-Al, Al-Si). The precision of our results is in the order of 15 to 25% relative error. The detection limits in our conditions are in the range of 30 (Ni, As, Sb) to 200 mg/kg (Ti, Fe, Zn, Sn, Ba, and Pb) for trace elements and in the range of 0.2 to 1% for major light elements. These detection limits were tested using NBS geological standards (W1, BM, KH). We analyzed approximately 150 Byzantine glass bracelets, the majority of them being different fragments, found in the same place: an ancient town on the border of Danube (North Dobroudja, approx. 100 km from Galatzi and 50 km near Danube Delta). We used XRF-PIXE for Z $\geq$ 19 (from K) and for Si, Al, Mg, Na – FNAA. We elaborated a list of "color receipts" as elemental chemical compositions with the purpose to help the archaeologists to classify the objects on provenance places (workshops), using literature data, and to obtain in this way information on various commercials and political aspects. A dedicated historical profile paper is under elaboration.

References

1. F. Tancu et al., *Rev. Roum. Phys.* 28(10), 857 (1983).
2. H. C. Evans and E. H. Bellamy, *Proc. Phys. Soc.* 74, 483 (1959).
3. R. J. Kurz, *Report UCRL* 11339 (1965).
4. M. A Lone et al., *Nucl. Instr. Meth.* 189, 515(1981).
5. A. Fabry and I. Garlea, *IAEA Report* 208 (2), 291(1978).
6. I. Grunde et al., *Nucl. Technology*, 25, 237 (1975).
7. A. McElroy et al., *Nucl. Sci. Eng.* 27, 533 (1967).
8. M. Stan et al., *Romanian Patent* 100648(1988).
9. L. Radu et al., *SPIE* 2461, 405 (1995).
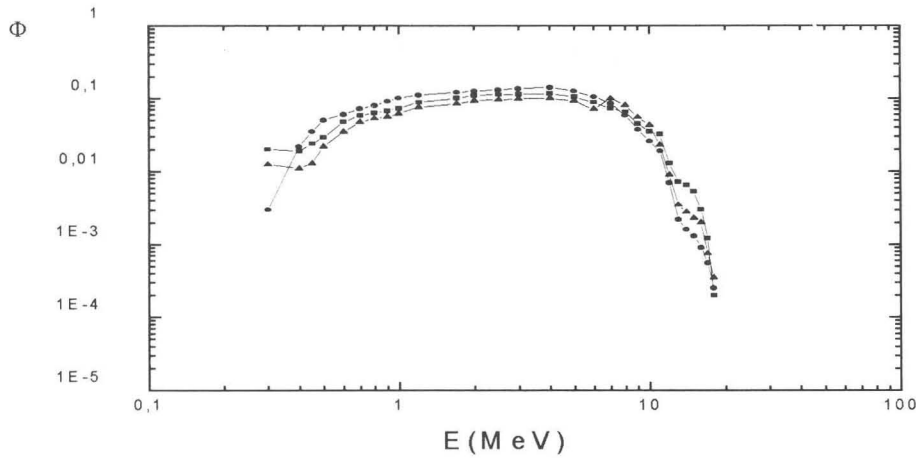10. B. Constantinescu et al., *J. Rad. Nucl. Chem. Letters*, 155(1), 25 (1991).

Figure 1. Normalized neutron spectra:

■   TOF, free-air;
●   Multiple foils method, free-air, 5 cm behind Be target;
▲   Multiple foils method, irradiation box, 10 cm behind Be target.

Table 1: Used radionuclides

Element	Nuclear reaction	Threshold (MeV)	Used nuclide	Half-life	Eγ(keV)
Mg	^{24}Mg(n,p)	4.93	^{24}Na	14.97h	1368.6
Al	^{27}Al(n,p)	1.9	^{27}Mg	9.45 min	1014
Si	^{29}Si(n,p)	3	^{29}Al	6.5 min	1273
K	^{41}K(n,p)	1.75	^{41}Ar	1.83h	1293.6
Ca	^{43}Ca(n,p)	1.06	^{43}K	22.3 h	373
	^{46}Ca(n,γ)	-	^{47}Ca	2.44d	271
Ti	^{46}Ti(n,p)	1.62	^{46}Sc	83.8d	889.3
	^{48}Ti(n,p)	3.27	^{48}Sc	43.7h	983.5
Fe	^{54}Fe(n,α)	-	^{51}Cr	27.7d	320.5
	^{54}Fe(n,p)	-	^{54}Mn	312.2d	834.5
Ni	^{58}Ni(n,p)	-	^{58}Co	70.91d	810.8
Cu	^{63}Cu(n,α)	-	^{60}Co	5.272y	1332.5
Zn	^{67}Zn(n,p)	-	^{67}Cu	61.9h	184.6
As	^{75}As(n,2n)	10.38	^{74}As	17.78d	595.9
Zr	^{90}Zr(n,2n)	12.07	^{89}Zr	78.4h	909.2
Ag	^{107}Ag(n,2n)	9.48	^{106}Ag	8.4d	451; 717
Cd	^{114}Cd(n,γ)	-	^{115}Cd	2.224d	336; 527
In	^{113}In(n,γ)	-	^{114m}In	49.5d	189.9
Sn	^{117}Sn(n,n')	-	^{117m}Sn	14d	158.5
	^{116}Sn(n,γ)	-	^{117m}Sn	14d	158.5
Sb	^{121}Sb(n,2n)	9.36	^{120m}Sb	5.76d	197; 1023
	^{121}Sb(n,γ)	-	^{122}Sb	2.72d	564
Ba	^{135}Ba(n,n')	-	^{135m}Ba	28.7h	268.2
	^{134}Ba(n,γ)	-	^{135m}Ba	28.7h	268.2
Pb	^{204}Pb(n,2n)	6.97	^{203}Pb	51.88h	279